Health: HL13306 and NS24067 to R.W.T., DA02121, DA02575, and MH40165 to R.J.M. E.W.M. was supported by a fellowship of the Muscular Dystrophy Association. L.D.H. and S.A.T. were supported by NIH National Research Service Awards DK07983 and NS08009, respectively. Additional support was also provided in part by The Miles Institute (R.W.T. and R.J.M.), the Brain Research Foundation, and Marion Laboratories (R.J.M.).

2 July 1987; accepted 20 October 1987

Molecular Crowding on the Cell Surface

T. A. RYAN, J. MYERS, D. HOLOWKA, B. BAIRD, W. W. WEBB

Strong steric interactions among proteins on crowded living cell surfaces were revealed by measurements of the equilibrium spatial distributions of proteins in applied potential gradients. The fraction of accessible surface occupied by mobile surface proteins can be accurately represented by including steric exclusion in the statistical thermodynamic analysis of the data. The analyses revealed enhanced, concentration-dependent activity coefficients, implying unanticipated thermodynamic activity even at typical cell surface receptor concentrations.

THE LATERAL DIFFUSIBILITIES OF most proteins in most cell surfaces have generally been found by fluorescence photobleaching recovery (FPR), postelectrophoresis relaxation (PER), and other techniques to be several orders of magnitude slower than predictable from simple hydrodynamic models, even though these models are appropriate for dilute protein concentrations in nearly pure lipid membranes (*1*). Comparisons with the rapid diffusibilities of proteins reconstituted into nearly pure lipid membranes (*2*) and in disrupted (bleb) membranes (*3*) have suggested that, in cells, interactions with the cytoskeleton, the glycocalix, or other cell surface proteins may constrain molecular diffusibility. Deletions of the cytoplasmic domains of certain cell surface receptors do not enhance their diffusibilities, suggesting that constraints other than direct anchorage to the cytoskeleton must exist (*4*). Interactions among the membrane proteins themselves have been inferred from the strong concentration dependence of the diffusibility of proteins reconstituted into artificial membranes (*2, 5*).

In an attempt to understand the nature of protein-protein interactions in cell membranes, we investigated the equilibrium properties of proteins on living cell surfaces. To avoid the complications of the dynamics of diffusion, we measured the equilibrium spatial distribution of fluorescence-labeled receptors on the surface of the nearly spherical rat basophilic leukemia (RBL) cells in an applied electric field. Previous measurements of the time course of PER have provided useful estimates of lateral molecular mobility (*6, 7*). In particular, the measurements of the diffusibilities of the immunoglobulin E receptor complex (IgER) on RBL cells were found to agree in PER and FPR experiments (*8, 9*).

Digital imaging microscopy (DIM) (*10, 11*) provides quantitative fluorescence images from which the distribution of fluorescence-labeled cell surface proteins can be measured accurately. Images of the asymmetric crowding of IgER on the surfaces of RBL cells induced by the electric field were analyzed in order to determine accurate maps of the receptor concentration on the cell surface (Figs. 1 and 2).

In an ideal solution, the equilibrium concentration distributions in a potential gradient can be described by a Boltzmann probability distribution over the potential energies ϵ

$$P(\epsilon) = \exp[-(\epsilon - \mu)/kT] \quad (1)$$

where μ is the chemical potential, k is the Boltzmann constant, and T is absolute temperature. On spherical cells of radius r in a uniform applied electric field E_0 (Fig. 2, inset), the potential energy ϵ of surface particles of effective charge Ze varies with angle θ relative to the applied field as (*12,13*)

$$\epsilon = (3/2)\, Zer \cos\theta \equiv \beta\cos\theta \quad (2)$$

Normalizing the distribution of mobile particles $C(\theta)$ to the initial (and average) concentration of mobile particles C_0 determines the chemical potential, such that the ideal distribution is given by

$$\frac{C(\theta)}{C_0} = \frac{2\beta}{kT} \cdot \frac{\exp[-\beta(1 + \cos\theta)/kT]}{1 - \exp(-2\beta/kT)} \quad (3)$$

Integration of Eq. 3 over all angles gives unity. Any immobile concentration C_{im} must be included in the total concentration $C_T(\theta)$ such that $C_T(\theta) = C(\theta) + C_{im}$ and $C_{0T} = C_0 + C_{im}$, where $C_{im} \equiv C_{0T}I_{im}$ defines an immobile fraction I_{im}. Previous measurements have been fit to a Boltzmann distribution (*7, 12*).

Fluorescence DIM experiments measure the total population $C_T(\theta)$ of labeled mobile and immobile proteins normalized to the initially uniform total concentration C_{0T}. Representative DIM measurements of the equilibrium distribution of fluorescein isothiocyanate (FITC)–labeled IgER on the surface of RBL cells after electrophoresis are shown in Fig. 2. Large discrepancies from the Boltzmann distribution curve are clearly evident (*14, 15*). The curve is forced to fit the data at low concentrations, emphasizing an obvious discrepancy that might be ascribed to saturation at high concentrations.

To account for saturation of the space on the cell membrane occupied by the proteins, we invoked simple steric exclusion. Analo-

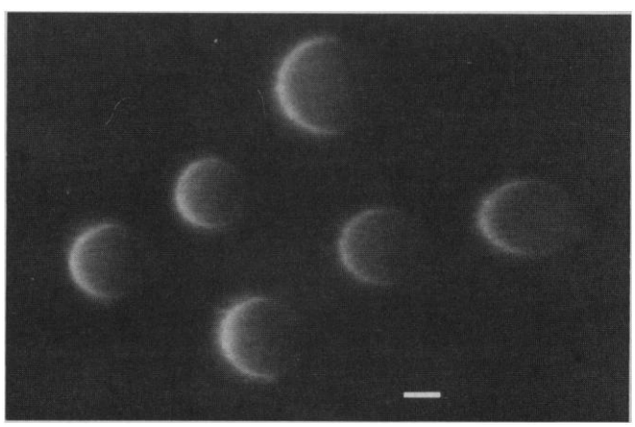

Fig. 1. The distribution of FITC-labeled IgER on the surface of live RBL cells (2H3 subline) after electrophoresis. Cells that were grown, harvested, and labeled with FITC-IgE as described (*8, 23*) were plated on No. 1 glass cover slips, mounted in an electrophoresis chamber (*24*) modified for an inverted microscope, and exposed to an applied electric field. Equilibrium of the surface distribution was verified by monitoring its time course after applying the field. Bar is 5 μm. All experiments were at room temperature unless otherwise noted.

T. A. Ryan, Department of Physics, Clark Hall, Cornell University, Ithaca, NY 14853.
J. Myers, D. Holowka, B. Baird, Department of Chemistry, Baker Laboratory, Cornell University, Ithaca, NY 14853.
W. W. Webb, School of Applied and Engineering Physics, Clark Hall, Cornell University, Ithaca, NY 14853.

gous exclusion principles generate the Fermi distribution and the Langmuir adsorption isotherm. We derived the equilibrium probability $P(\epsilon)$ of finding an electrochemically mobile molecule at a potential energy ϵ relative to the chemical potential μ and found that it is a Fermi distribution:

$$P(\epsilon) = \frac{\exp[-(\epsilon - \mu)/kT]}{1 + \exp[-(\epsilon - \mu)/kT]} \quad (4)$$

The denominator expresses the effect of steric exclusion.

Now, in the absence of a field, a uniform equilibrium concentration C_0 of all mobile cell surface proteins occupies a fraction $f_0 = C_0/C_S$ of all accessible surface sites of concentration C_S. Applying Eq. 4 to this population determines an initial chemical potential μ_0 when $\epsilon = 0$ everywhere, such that

$$f_0 = \frac{C_0}{C_S} = \frac{\exp(\mu_0/kT)}{1 + \exp(\mu_0/kT)} \quad (5)$$

In the applied field, the mobile population again reaches an equilibrium among the accessible sites of density ρ at energies ϵ with probability $P(\epsilon)$, and the chemical potential μ shifts to conserve the mean concentration $\langle C \rangle = C_0$ such that

$$\int_{\epsilon} P(\epsilon)\rho d\epsilon = C_0 \quad (6)$$

On spherical cells, $\rho = C_0/2\beta f_0$ and $\epsilon = \beta\cos\theta$ (Eq. 2), just as for the Boltzmann distribution, and the angle-dependent concentration $C(\theta) = P(\theta)2\beta\rho$. The position-dependent fractional occupancy $f(\theta) \equiv P(\theta) = C(\theta)/C_S$. The surface average of f is f_0. Solving Eq. 6 for the chemical potential of the redistributed mobile proteins in the applied field yields

$$\exp(\mu/kT) = \frac{\exp(\beta/kT) - \exp[\beta(1 - 2f_0)/kT}{\exp[2\beta(1 - f_0)/kT] - 1} \quad (7)$$

Equation 4 with Eqs. 2 and 7 provides the equilibrium concentration distributions $C(\theta)$ in the applied field. Assuming a fraction of labeled proteins I_{im} that are immobile in the electric field, we obtain

$$\frac{C_T(\theta)}{C_{0T}} = f(\theta)\frac{C_S}{C_{0T}} + I_{im} = \frac{(1 - I_{im})/f_0}{\exp(\beta\cos\theta/kT)\exp(-\mu/kT) + 1} + I_{im} \quad (8)$$

The sites occupied by the immobile fraction I_{im} are by definition inaccessible. The crowding model can be tested by fitting Eq. 8 to measurements of protein distributions induced by electric fields on cell surfaces like those shown in Figs. 1 and 2.

Detailed measurements of the equilibrium redistributions in applied fields of the fluorescence-labeled IgER complexes are presented in Fig. 3A. They are fit by Eq. 8 at all values of θ. The three fitting parameters f_0, β, and I_{im} determined for each of these experiments at four applied fields are reported in Table 1. They show an average occupancy of accessible sites $f_0 \simeq 45\%$ and an immobile fraction $I_{im} \simeq 30\%$ in each case. As required, f_0 and I_{im} are independent of E_0. The values of β vary linearly with applied field strength E_0, as required (Fig. 3B); the slope $d\beta/dE_0$ yields an effective unit charge number $Z \simeq 5.5$ with a standard error of ± 2.0.

In the highest field applied in these experiments, the fraction of accessible surface occupied by mobile proteins $f(\theta)$ increased at the cathodal pole to $f_{max} \approx 70\%$ and decreased at the depleted anodal pole to $f_{min} \approx 5\%$. Because the essential parameters f_0, Z, and I_{im} are independent of E_0, they should be the same everywhere on the cell surface in applied fields up to at least 20 V/cm.

The parameters $f_0 = C_0/C_S$ and $\beta = (3/2)ZerE_0$ are supposed to represent the complete mobile protein population, but IgER is thought to comprise only $\simeq 1\%$ of the total surface protein on RBL cells (*16*). Therefore, it was necessary to demonstrate that IgER is a representative marker of the entire general population of mobile surface proteins, as is assumed in the crowding theory underlying Eqs. 4 to 8. To test this, we measured the equilibrium concentration profiles in electric potential gradients on these RBL cells for two different nonspecific

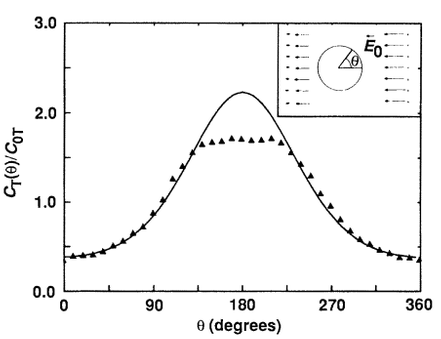

Fig. 2. Relative surface concentration profile $C_T(\theta)/C_{0T}$ of IgER on RBL cells equilibrated in an applied field of 15 V/cm. The ratio $C_T(\theta)/C_{0T}$ is displayed as a function of angle θ with respect to direction of the applied field E_0 (see inset). The standard deviation of the mean values for the data points shown was typically $\sigma \simeq 10\%$ of the mean. The solid line is an attempted fit to Boltzmann statistics, including an immobile fraction. The fluorescence intensity of the ring stain of cells chosen for circular peripheries at equatorial focus were recorded at 10° intervals after background subtraction (*15*). The scans of typically 25 to 50 cells were normalized and combined to produce an ensemble average measurement of the relative surface concentration profile $[C_T(\theta)/C_{0T}]$ (shown is an average of $\simeq 30$ cells). All experiments repeated on several different days with different cell preparations were consistent within the error of measurement. The digital fluorescence images of the distribution of fluorescence-labeled proteins on the surface of RBL cells were recorded with a 100× Neofluar 1.3 NA oil objective on an inverted epi-illuminated fluorescence microscope (Zeiss IM-35) (with appropriate excitation-dichroic-barrier filter combinations for fluorescein or rhodamine) coupled to an intensified video camera (Venus Scientific TV2 or TV3). Neutral density filters were used in the optical path of the excitation source (a 100-watt mercury arc lamp) to maintain the fluorescence intensity within the linear range of the camera. Photobleaching was negligible. The images were digitized and typically averaged over 30 frames in a Trapix 5500 image processor (Recognition Concepts, Inc.).

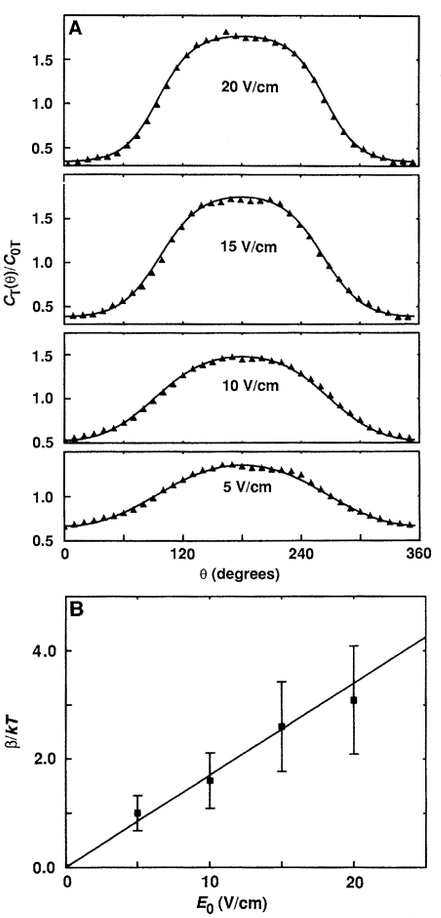

Fig. 3. (**A**) Equilibrium relative cell surface concentration profiles of IgER on RBL cells in applied electric fields fit by the steric exclusion theory for crowding (Eq. 8). $C_T(\theta)/C_{0T}$ is plotted for angle θ with respect to E_0. At each E_0, the data set was fit independently to Eq. 8 to determine β, I_{im}, and f_0 by a nonlinear least-squares procedure. (**B**) Values of the fitted electrochemical potential factors $\beta/kT = 3ZerE_0/2kT$ as a function of the applied electric field strength E_0; the slope gives the effective charge number.

labels of the surface protein distribution. Measurements were made on populations of cells that were labeled postelectrophoretically with (i) TRITC-S–Con A, which binds primarily to α-D-mannose glycoproteins or with (ii) a fluorescence-conjugated polyclonal antibody raised against the plasma membranes of RBL cells (*17*). Both equilibrium distributions of the mobile fractions of labeled proteins were redistributed in the electrical potential gradient just like IgER (Fig. 4). All values of $f_0 \simeq 45\%$ agree (Table 1), indicating that the same areas are accessible to all mobile proteins as had been implicitly assumed despite the larger, variable immobile fractions I_{im}. The same effective unit charge $Z \simeq 5.5 \pm 2$ was obtained from the values of β for each marker, again as assumed.

As known from FPR and PER experiments, some of the observed cell surface protein may comprise an electro-immobile fraction of the population I_{im}, which appears as the offset in Eq. 8. The fraction $F = f_0/[1 - I_{im}(1 - f_0)]$ of total sites effectively covered by some protein appears to be about 75% if the immobile sites are saturated. F consists of two parts: (i) the area covered by all immobile proteins I_{im}, which is inaccessible to mobile molecules, and (ii) the fraction f of the accessible area that is occupied by mobile proteins. The values of the immobile fractions I_{im} we find vary strongly with surface particle but are generally similar to values obtained by FPR. No field dependence of I_{im} was detected, so we conclude that immobile proteins were not dislodged by the electrostatic forces in these experiments. Cell surface rugosities like microvilli blur the definition of the true surface area and probably modify the immobile fractions; our fractions are defined in terms of projected areas.

The results of our theory of crowding of the cell surface protein can be described by a relative activity coefficient $\gamma \equiv 1/(1 - f)$, which is convenient for estimating thermodynamic effects. The ratio of the concentrations at equal electrochemical potentials $\mu + \epsilon$ for ideal solution theory (Boltzmann distribution, Eq. 1) and for our excluded area theory (Fermi distribution, Eq. 4) defines γ. In our analysis, $\gamma \simeq 2$ at normal cell surfaces and rises to $\gamma \simeq 4$ at our highest concentration. These results imply support for theoretical models of cooperative protein-protein interactions arising from crowding in both aqueous solutions (*18*) and model membranes (*19*).

The effects of crowding on diffusion in either two or three dimensions appear ubiquitous. A strong dependence on spatial scale for the diffusivities of hard spheres in dense liquid suspensions has been found, such that diffusion at high concentration over many sphere diameters is slowed by several orders of magnitude relative to short scales and to the low concentration limit (*20*). In reconstituted membranes, high protein-to-lipid ratios have been shown to slow lateral diffusion of both bacterial rhodopsin and gramicidin C (*2*). Although theoretical modeling suggests that large immobile fractions as well as high concentrations of mobile particles can slow diffusion by orders of magnitude in two-dimensional systems (*21*), the effect of the steric interaction on the thermodynamic activity would be to increase the driving forces and thus to speed diffusion. Diffusion on the crowded cell membrane remains a problem to be resolved.

In summary, we find that proteins on the surface of living cells do not behave as ideal solutes in the lipid membrane. Instead, crowding of surface proteins enhances the thermodynamic activities of mobile surface proteins in accord with a simple theory leading to a Fermi distribution. These effects may be ubiquitous features of cell surfaces (*22*) and are likely to have profound effects on cell surface receptor action.

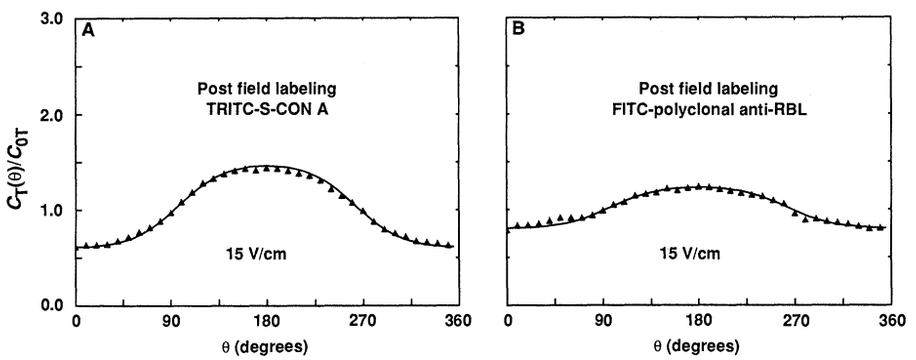

Fig. 4. Equilibrium relative surface concentration profiles in applied electric fields for two nonspecific labels. Data are averages of measurements of ≃50 RBL cells that were exposed to an external electric field E_0 = 15 V/cm for 40 minutes (equilibrium was reached in ≃25 minutes), rapidly cooled to 4°C [to avoid relaxation; (*9*)], and labeled for 30 minutes at 4°C with either (**A**) 50 μg/ml tetramethylrhodamine isothiocyanate succinyl concanavalin A (TRITC-S–Con A) (E-Y Labs, Inc.) or (**B**) 5 μg/ml FITC-modified polyclonal antibody raised against the RBL cell membrane (*17*). The cells were then washed and rapidly fixed in 4°C acetone for 45 seconds, rinsed three times with phosphate-buffered saline, and mounted for observation. The solid lines are results of best nonlinear least-squares fit to Eq. 8.

Table 1. Fitting parameters with the steric exclusion principle. Mean values of fitting parameters β, f_0, and I_{im} for all measurements obtained from nonlinear least-squares fit to Eq. 8 are presented. The quoted errors are of standard errors in the means obtained for all individual cells of a set on a given day. Variations from day to day were less than the variations from cell to cell on a given day.

Labeled protein	β/kT	f_0 (%)	I_{im} (%)	E_0 (V/cm)
FITC-IgER	1.00 ± 0.32	45 ± 7	30 ± 15	5
	1.60 ± 0.51	43 ± 7	31 ± 15	10
	2.57 ± 0.82	49 ± 8	30 ± 15	15
	3.09 ± 0.98	46 ± 7	30 ± 15	20
TRITC-S–Con A*	2.22 ± 1.40	43 ± 14	54 ± 22	15
FITC–anti-RBL*	2.20 ± 1.40	43 ± 14	77 ± 31	15

*Labeled after electrophoresis (Fig. 4).

REFERENCES AND NOTES

1. M. McCloskey and M-M. Poo, *Int. Rev. Cytol.* **87**, 19 (1984); K. Jacobson, A. Ishihara, R. Inman, *Annu. Rev. Physiol.* **49**, 163 (1987); K. Jacobson, E. Elson, D. Koppel, W. Webb, *Nature (London)* **295**, 283 (1982); *Fed. Proc. Fed. Am. Soc. Exp. Biol.* **42**, 72 (1983); E. L. Elson, *Annu. Rev. Phys. Chem.* **36**, 379 (1985); R. J. Cherry, *Biochem. Biophys. Acta* **559**, 289 (1979); R. Peters, *Cell. Biol. Int. Rep.* **5**, 733 (1981); M. Edidin, in *New Comprehensive Biochemistry*, J. B. Finean and R. H. Mitchell, Eds. (Elsevier, Amsterdam, 1981), vol. 1, pp. 37–82.
2. D. W. Tank, E.-S. Wu, P. R. Meers, W. W. Webb, *Biophys. J.* **40**, 129 (1982); W. L. C. Vaz, M. Criado, V. M. Madiera, G. Schoellmann, T. Jovin, *Biochemistry* **21**, 5608 (1982); R. Peters and R. J. Cherry, *Proc. Natl. Acad. Sci. U.S.A.* **79**, 4317 (1982).
3. E.-S. Wu, D. W. Tank, W. W. Webb, *Proc. Natl. Acad. Sci. U.S.A.* **79**, 4962 (1982); D. W. Tank, E.-S. Wu, W. W. Webb, *J. Cell Biol.* **92**, 207 (1982); W. W. Webb, L. S. Barak, D. W. Tank, E.-S. Wu, *Biochem. Soc. Symp.* **46**, 191 (1981).
4. B. F. Scullion, Y. Hou, L. Puddington, J. K. Rose, K. Jacobson, *J. Cell Biol.* **105**, 69 (1987); E. Livneh *et al.*, *ibid.* **103**, 327 (1986); R. Ghosh and W. W. Webb, unpublished data; M. Edidin and M. Zuniga, *J. Cell Biol.* **99**, 2333 (1984).
5. W. L. C. Vaz, F. Goodsaid-Zalduando, K. Jacobson, *FEBS Lett.* **174**, 199 (1984).
6. M-M. Poo, *Annu. Rev. Biophys. Bioeng.* **10**, 245 (1981).
7. D. W. Tank, W. J. Fredericks, L. S. Barak, W. W. Webb, *J. Cell Biol.* **101**, 148 (1985).

8. D. Wolf, M. Edidin, P. R. Dragsten, *Proc. Natl. Acad. Sci. U.S.A.* 77, 2043 (1980); A. K. Menon, D. Holowka, W. W. Webb, B. Baird, *J. Cell Biol.* **102**, 534 (1986); A. K. Menon, D. Holowka, W. W. Webb, B. Baird, *ibid.*, p. 541.
9. M. McCloskey, Z-Y. Liu, M-M. Poo, *J. Cell Biol.* **99**, 778 (1984).
10. D. J. Arndt-Jovin, M. Robert-Nicaud, S. J. Kaufman, T. M. Jovin, *Science* **230**, 247 (1985).
11. D. Gross, L. M. Loew, W. W. Webb, *Biophys. J.* **50**, 339 (1986).
12. M-M. Poo, J. W. Lam, N. Orida, A. W. Chao, *ibid.* **26**, 1 (1979).
13. The numerical factor of 3/2 applies to virtually impermeable cells that exclude external fields; as fields penetrate, the factor decreases to 1 (*11*).
14. Self-quenching of fluorescein chromophores by resonance energy transfer or collisions cannot account for the observed results. In fact, extensive cross-linking of FITC-IgER complexes to each other by IgE antiserum does not cause measurable quenching of fluorescein fluorescence (A. K. Menon, D. Holowka, B. Baird, in preparation).
15. The measured fluorescence intensities represent convolution integrations of the source with the instrument point spread function along the optical axis of the microscope. Convolutions of an approximate Gaussian instrumental function with trial fluorescence distributions on the surface of a spherical cell (Eq. 8) showed that the out-of-focus contributions to the measured intensities result in negligible underestimates of f_0 and β by a few percent and an overestimate of I_{im} by a few percent. Our cells are slightly flattened, but the adequacy of the spherical approximation was verified.
16. D. Holowka, unpublished observations based on surface-labeling studies.
17. C. Isersky, G. R. Mendoza, H. Metzger, *J. Immunol.* **119**, 123 (1977). The polyclonal antibody was prepared in the laboratory of C. Isersky.
18. A. Minton, *Mol. Cell. Biochem.* **55**, 119 (1983).
19. B. Grasberger, A. P. Minton, C. DeLisi, H. Metzger, *Proc. Natl. Acad. Sci. U.S.A.* **83**, 6258 (1986).
20. R. M. Ottewill and N. St. J. Williams, *Nature (London)* **325**, 232 (1987).
21. M. Saxton, *Biophys. J.* **39**, 165 (1982); P. N. Pusey, in *Physics of Amphiphiles: Micelles, Vesicles and Microemulsions*, V. DeGiorgio and M. Corti, Eds. (North-Holland, Amsterdam, 1985); J. Eisinger, J. Flores, W. P. Petersen, *Biophys. J.* **49**, 987 (1986); M. J. Saxton, *ibid.* **51**, 542a (1987); J. R. Abney, B. A. Scalettar, J. C. Owicki, *ibid.*, p. 541a.
22. Since the structure [C. Isersky, J. Rivera, T. J. Triche, H. Metzger, *Mol. Immunol.* **19**, 925 (1982)] and function [H. Metzger *et al.*, *Annu. Rev. Immunol.* **4**, 419 (1986)] of RBL plasma membranes appear to be typical of eukaryotic cells, their cell surface receptor properties should be representative of a large class of cell types.
23. J. D. Taurog, C. Fewtrell, E. Becker, *J. Immunol.* **122**, 2150 (1979); E. L. Barsumian, C. Isersky, M. G. Petrino, R. Siraganian, *Eur. J. Immunol.* **11**, 317 (1981).
24. D. Gross, L. M. Loew, T. A. Ryan, W. W. Webb, in *Ionic Currents in Development*, R. Nuccitelli, Ed. (Liss, New York, 1986), pp. 263–270.
25. We thank J. Rivera and H. Metzger for providing the polyclonal antibody to RBL membranes. Supported by ONR N00014-84-K-0390, NSF DMB-8609084, and NIH GM33028 to T.A.R. and W.W.W.; NIH-AI18306 and NIH-AI22449 to J.M., D.H., and B.B.; and the Cornell Biotechnology Program, which is sponsored by the New York State Science and Technology Foundation and a consortium of industries.

28 August 1987; accepted 30 November 1987

Human Ribosomal RNA Genes: Orientation of the Tandem Array and Conservation of the 5′ End

RONALD G. WORTON,* JOANNE SUTHERLAND,† JAMES E. SYLVESTER, HUNTINGTON F. WILLARD, SHARON BODRUG, IAN DUBÉ,‡ CATHERINE DUFF, VANORA KEAN,§ PETER N. RAY, ROY D. SCHMICKEL

The multiple copies of the human ribosomal RNA genes (rDNA) are arranged as tandem repeat clusters that map to the middle of the short arms of chromosomes 13, 14, 15, 21, and 22. Concerted evolution of the gene family is thought to be mediated by interchromosomal recombination between rDNA repeat units, but such events would also result in conservation of the sequences distal to the rDNA on these five pairs of chromosomes. To test this possibility, a DNA fragment spanning the junction between rDNA and distal flanking sequence has been cloned and characterized. Restriction maps, sequence data, and gene mapping studies demonstrate that (i) the rRNA genes are transcribed in a telomere-to-centromere direction, (ii) the 5′ end of the cluster and the adjacent non-rDNA sequences are conserved on the five pairs of chromosomes, and (iii) the 5′ end of the cluster is positioned about 3.7 kb upstream from the transcription initiation site of the first repeat unit. The data support a model of concerted evolution by interchromosomal recombination.

HUMAN DIPLOID CELLS CONTAIN 300 to 400 copies of the genes encoding 18*S* and 28*S* ribosomal RNA (rRNA) (*1*), occurring in blocks of tandemly repeated genes on the short arms of the five pairs (numbers 13, 14, 15, 21, and 22) of acrocentric chromosomes (*2*). Each rRNA gene block (rDNA) lies within the uniquely staining nucleolus organizer region (NOR) (*3*), flanked on the proximal (centromere) and distal (telomere) side by a region of non-rDNA. The 44-kb rDNA repeat unit (Fig. 1) contains a 13-kb transcribed portion and a 31-kb nontranscribed spacer (*4*). The 13-kb RNA transcript is processed to yield the 18*S*, 5.8*S*, and 28*S* mature rRNA molecules. Within a block of rDNA, the repeat units are tandemly arranged in a head-to-tail fashion but the orientation of this cluster on the acrocentric chromosomes has not previously been determined. Little information has been available on the borders of the cluster. In particular, the end unit and adjacent sequence have not been identified, and it is not known whether these end points are conserved among the five acrocentric chromosomes or among individuals in the population. The identification of an X-autosome translocation involving ribosomal RNA genes has allowed us to determine the orientation of the rDNA complex on the acrocentric chromosomes and to clone DNA sequences from the junction of rDNA with sequences on the telomeric side.

The unique translocation t(X;21) (p21;p12) (Fig. 1, inset) between the X chromosome and chromosome 21 was ascertained in a girl with X-linked muscular dystrophy (*5*). The exchange point in the X chromosome is at the muscular dystrophy locus in band Xp21 and the rearrangement is responsible for the disease (*6*). The exchange point in chromosome 21 was mapped cytologically within the rDNA block at band 21p12 (*5*) and molecular analysis revealed that three to five copies of rDNA plus the distal end of chromosome 21 were translocated to the X-derived translocation chromosome, der(X), while 40 to 60 copies of rDNA remained on the chromosome 21–derived translocation chromosome, der(21) (*7*).

These studies were greatly facilitated by the availability of somatic cell hybrid lines containing the der(X) chromosome (hybrid A2) and the der(21) chromosome (hybrid B2), free of other human acrocentric chromosomes (*7*). The estimate of the number of copies of rDNA on der(X) came from quan-

R. G. Worton, H. F. Willard, S. Bodrug, Genetics Department and Research Institute, Hospital for Sick Children, Toronto M5G 1X8, and Department of Medical Genetics, University of Toronto, Toronto, Ontario, Canada.
J. Sutherland, I. Dubé, C. Duff, V. Kean, P. N. Ray, Genetics Department and Research Institute, Hospital for Sick Children, Toronto, Ontario, Canada M5G 1X8.
J. E. Sylvester and R. D. Schmickel, Department of Human Genetics, University of Pennsylvania, Philadelphia, PA 19104.

*To whom correspondence should be addressed.
†Present address: Genetics Department, Children's Psychiatric Research Institute and Children's Hospital of Western Ontario, London, Ontario, Canada.
‡Present address: Department of Pathology, Toronto General Hospital, Toronto, Ontario, Canada.
§Present address: Molecular Neurobiology Laboratory, Department of Ophthalmic Optics, University of Manchester Institute of Science and Technology, Manchester, United Kingdom.